IOPscience iopscience.iop.org

Home Search Collections Journals About Contact us My IOPscience

Physical properties of asymmetric photonic crystal waveguides

This content has been downloaded from IOPscience. Please scroll down to see the full text.

2009 J. Opt. A: Pure Appl. Opt. 11 015103

(http://iopscience.iop.org/1464-4258/11/1/015103)

View the table of contents for this issue, or go to the journal homepage for more

Download details:

IP Address: 140.113.38.11
This content was downloaded on 25/04/2014 at 13:39

Please note that terms and conditions apply.

J. Opt. A: Pure Appl. Opt. **11** (2009) 015103 (6pp) doi:10.1088/1464-4258/11/1/015103

Physical properties of asymmetric photonic crystal waveguides

Chih-Hsien Huang[1], **Wen-Feng Hsieh**[1] **and Szu-Cheng Cheng**[2]

[1] Department of Photonics and Institute of Electro-Optical Engineering, National Chiao Tung University, 1001 Tahsueh Road, Hsinchu, Taiwan
[2] Department of Physics, Chinese Culture University, Taipei, Taiwan

E-mail: wfhsieh@mail.nctu.edu.tw and sccheng@faculty.pccu.edu.tw

Received 22 July 2008, accepted for publication 10 November 2008
Published 4 December 2008
Online at stacks.iop.org/JOptA/11/015103

Abstract
By considering the next nearest neighboring defects between two photonic crystal waveguides (PCWs) and analytic formulae derived from the tight binding theory, we will explain the physical properties of an asymmetric directional coupler made from two coupled PCWS: (1) The dispersion curves of a photonic crystal coupler will decouple into the dispersion curves of a single line defect, and the electric field will only be localized in one waveguide of the coupler at a particular point, which we name a decoupling point. (2) The parities of the eigenmodes switch at the decoupling point, even though the dispersion curves are not crossing. (3) The eigenfield at a higher (lower) dispersion curve is always mainly localized in the waveguides that have higher (lower) eigenfrequencies of single line defects, even though the eigenmodes are switched. As a given frequency is incident into the coupler, the energy transfer between two waveguides and the coupling length can be expressed analytically. Due to there being no dispersion curve crossing, the coupling length is no longer infinite at the decoupling point in asymmetric PCWs, but it still has the minimal energy transfer between two waveguides when the frequency of the incident wave is close to the decoupling point.

Keywords: directional coupler, defects, tight-binding model

(Some figures in this article are in colour only in the electronic version)

1. Introduction

A photonic crystal waveguide (PCW) is a structure in which a series of point defects are created within the photonic crystal (PC) [1]. The electromagnetic (EM) wave is strongly confined along the defect channel, where low loss of energy in Y-branches and tight bending are possible [2]. Furthermore, directional couplers each composed of two line defects are used as add/drop filters [3], switches [4], and multiplexers [5]. To design the PC devices, simulation tools such as the plane wave expansion (PWEM) [6–8] and finite difference time domain (FDTD) [9–11] methods are often used. However, there still is no efficient and analytic method for analyzing the physical properties of the PC waveguides (PCWs), especially for the directional coupler. The tight binding theory (TBT) is widely used, not only in condensed matter physics but also recently analytically to address the EM wave propagation in a linear or nonlinear PCW [12–14]. TBT usually takes into account the coupling between nearest neighboring defects and ignores further coupling between distant defects. Although this approximation is valid for coupled cavity waveguides, it is invalid for PCWs, where the coupling between next nearest neighboring defects should be considered within a single waveguide and between two waveguides [15]. The cross-coupling coefficient (α) of the nearest neighbors between two waveguides causes a split of the dispersion curves, whereas the cross-coupling coefficient (β) of the next nearest neighbor causes a sinusoidal modulation of the dispersion curves in symmetric PCWs. The split dispersion curves will cross in symmetric PCWs if $|2\beta/\alpha| > 1$. At the crossing point, the coupling length that can be used to design dual-wavelength demultiplexing is infinite [16, 17].

On changing the radii or dielectric constants of the defect rods in one channel of the PCWs, the symmetry of the PCWs

 © 2009 IOP Publishing Ltd Printed in the UK

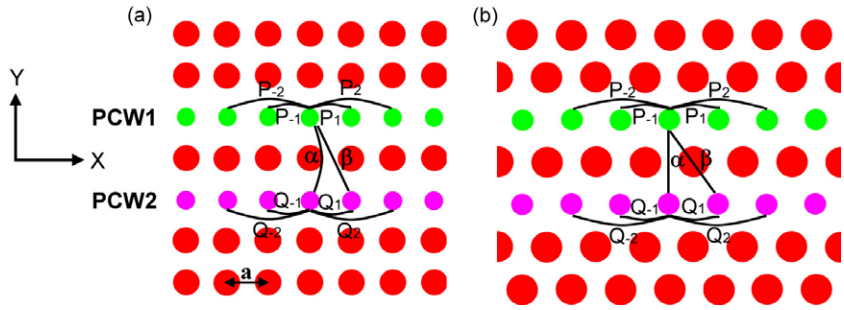

Figure 1. Geometric structures of the photonic crystal waveguide couplers of (a) a square lattice and (b) a triangular lattice with the lattice constant a. P_s and Q_s are the coefficients of coupling between defects within a single waveguide. α, and β are the coefficients of coupling between waveguides.

will be broken. From the simulation results for the PWEM for the triangular lattice, the dispersion curves of asymmetric PCWs are not crossing, but the eigenmodes do switch. The electric field ratios of the eigenmodes in both waveguides are no longer ± 1, especially at the switching point of the mode pattern (figure 3). However, the results for the PWEM or TBT derived from symmetric PCWs cannot provide good reasons for explaining these phenomena. Therefore, using a method similar to the tight binding one [15, 18, 19], we derive an analytic solution considering up to the next neighbor coupling between two PCWs to describe the physical properties of asymmetric PCWs. This formula provides more generalized discussion and gives a good explanation for asymmetric PCWs. In practice, the coupled identical PCWs should become asymmetric due to the intensity dependent index of refraction in the nonlinear photonic crystal directional coupler, and this can be used in switches for controlling EM waves to the output with the proper ratio in each channel.

In this paper, we first use TBT to derive the analytic expressions for the dispersion relation and eigenmodes of a directional coupler with two asymmetric PCWs. On the basis of the derived equations and the definition of the coupling coefficients, the mode switching, mode parity, and electric field distribution are discussed. Here, we consider only the PCs formed from dielectric rods in air as an example, and two line defects created by reducing the radii of the dielectric rods as the waveguides. The derived TBT is also applicable for airhole PCs with the enlarged airholes as the line defect PCWs, in order to preserve a single-mode property in each of the PCWs. However, the TBT derived in this paper may not be suitable for a PC directional coupler formed from dielectric defect PCWs, which were created by increasing the radii of the dielectric rods or by decreasing the radii of the airholes, although switching of eigenmodes can also be observed, because the dielectric defect PCWs would sustain multi-guided modes [20].

Secondly, by superimposing these two eigenmodes of the asymmetric PCW at a given frequency, electric field amplitudes of individual PCWs can also be obtained by deriving the coupling length and the ratio of the energy transfer. Finally, the PCWs of the triangular lattice are used to verify the validity of the derived expressions and the predicted physical properties. The results derived from the TBT coincide quite well with the PWEM results. Therefore, TBT is a good method for analytically characterizing the coupling phenomena of asymmetric PCWs.

2. Coupled equations of asymmetric photonic crystal waveguides

The asymmetric coupled PCWs in a PC with the lattice constant a are formed from two rows of periodic defect rods partitioned by a perfect row of rods, shown as PCW1 and PCW2 in figure 1 for the square and the triangular lattices, respectively. To ensure that the PCWs are both single-mode waveguides, we simply reduce the radii of the dielectric rods or decrease the refractive indexes of the rods. The field distribution of the eigenmode of an isolated (point) defect in each PCW can be written as the product of time varying and spatially varying functions, i.e., $\mathbf{E}_{10}(\mathbf{r}, t) = u_0(t)\mathbf{E}_{10}(\mathbf{r})$ in PCW1 and $\mathbf{E}_{20}(\mathbf{r}, t) = v_0(t)\mathbf{E}_{20}(\mathbf{r})$ in PCW2, where $u_0(t) = U' \exp(-\mathrm{i}\omega_1 t)$ and $v_0(t) = V' \exp(-\mathrm{i}\omega_2 t)$, with U' and V' being the constant amplitudes of the electric fields and ω_1 and ω_2 the frequencies of the localized modes of the point defect in each PCW.

Under the TBT, the propagating electric field of PCW1 can be expanded in terms of the localized fields of the individual point defects as $\mathbf{E}_1(\mathbf{r}, t) = \sum_n \mathbf{E}_{1n}(\mathbf{r})u_n(t)$. Here, $\mathbf{E}_{1n}(\mathbf{r}) = \mathbf{E}_{10}(\mathbf{r} - na\hat{x})$ is the localized electric field at the defect site n and $u_n(t)$ is its time varying function. Considering the coupling by means of the Lorentz reciprocity relation [21], the evolution equation of the isolated PCW1 can be written as

$$\mathrm{i}\frac{\partial}{\partial t}u_n = (\omega_1 - P_0)u_n - \sum_{m=1} P_m(u_{n+m} + u_{n-m}) \qquad (1)$$

and $P_m = C_m^{11}$, where C_m^{ij} is the coefficient of coupling between the site n of the ith PCW and the site $n + m$ of the jth PCW, and is defined as

$$C_m^{ij} = \frac{\omega_i \int_{-\infty}^{\infty} \mathrm{d}v\, \Delta\varepsilon(\mathbf{r})\mathbf{E}_{\mathrm{in}} \cdot \mathbf{E}_{jn+m}}{\int_{-\infty}^{\infty} \mathrm{d}v[\mu_0|\mathbf{H}_{\mathrm{in}}|^2 + \varepsilon|\mathbf{E}_{\mathrm{in}}|^2]}. \qquad (2)$$

$\Delta\varepsilon(\mathbf{r}) = \varepsilon'(\mathbf{r}) - \varepsilon(\mathbf{r})$ is the difference between the perturbed and unperturbed dielectric constants, and P_0 represents the frequency shift of a localized mode due to the change of the dielectric constant at the site n of the first PCW. In general,

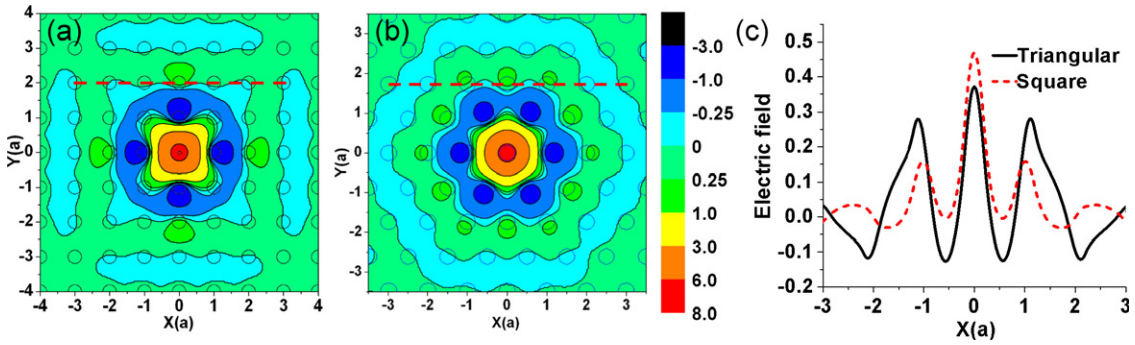

Figure 2. (a) The electric field distribution (E_z) of a point defect mode in the square lattice for $f = 0.364c/a$ with a reduced rod ($r_d = 0.05a$) defect; (b) that in the triangular lattice for eigenfrequency $f = 0.365c/a$ with a defect rod $\varepsilon_r = 2.56$; and (c) the electric field distribution (dashed lines).

the electric field at the defect rods that are fourth neighbors is almost zero, so considering the coupling coefficients P_m up to $m = 3$ is quite enough [15]. Let k and $\bar{\omega}_1$ be the wavevector and its corresponding eigenfrequency for PCW1, respectively. We then substitute the function $u_n(t) = U_0 \exp(\mathrm{i}kna - \mathrm{i}\bar{\omega}_1 t)$ into equation (1) and obtain the dispersion relation for PCW1:

$$\bar{\omega}_1(k) = \omega_1 - P_0 - \sum_{m=1}^{3} 2P_m \cos(mka), \tag{3}$$

where U_0 is a constant. Similarly, the evolution equation and dispersion relation for the isolated PCW2 are as shown below:

$$\mathrm{i}\frac{\partial}{\partial t}v_n = (\omega_2 - Q_0)v_n - \sum_{m=1}^{3} Q_m(v_{n+m} + v_{n-m}), \tag{4}$$

$$\bar{\omega}_2(k) = \omega_2 - Q_0 - \sum_{m=1}^{3} 2Q_m \cos(mka), \tag{5}$$

where $Q_m = C_m^{22}$. $v_n(t)$ and $\bar{\omega}_2$ are the time varying function and the eigenfrequency of the isolated PCW2, respectively.

Due to the field distributions of defect modes being not strongly localized around defects, we shall consider the effect of coupling of two asymmetric PCWs up to the defects that are second neighbors, with coupling coefficients $\alpha = C_0^{12} = C_0^{21}$ and $\beta = C_{\pm1}^{12} = C_{\pm1}^{21}$, shown in figure 1 for the square and the triangular lattices, respectively. The coupled equations for asymmetric PCWs are given by

$$\mathrm{i}\frac{\partial}{\partial t}u_n = (\omega_1 - P_0)u_n - \sum_{m=1}^{3} P_m(u_{n+m} + u_{n-m}) - \alpha v_n - \beta(v_{n+1} + v_{n-1}), \tag{6}$$

$$\mathrm{i}\frac{\partial}{\partial t}v_n = (\omega_2 - Q_0)v_n - \sum_{m=1}^{3} Q_m(v_{n+m} + v_{n-m}) - \alpha u_n - \beta(u_{n+1} + u_{n-1}). \tag{7}$$

The stationary solutions of coupled equations (6) and (7) are taken as $u_n = U_0 \exp(\mathrm{i}kna - \mathrm{i}\omega t)$ and $v_n = V_0 \exp(\mathrm{i}kna - \mathrm{i}\omega t)$. We obtain the characteristic equations of the coupler:

$$(\omega - \bar{\omega}_1)U_0 + g(ka)V_0 = 0, \tag{8}$$

$$(\omega - \bar{\omega}_2)V_0 + g(ka)U_0 = 0, \tag{9}$$

where $g(ka) = \alpha + 2\beta\cos(ka)$ and $\begin{bmatrix} U_0 \\ V_0 \end{bmatrix}$ stands for the eigenvector or field amplitude in the two PCWs. The eigenfrequencies (dispersion relations) and eigenvectors (field amplitudes) of equations (8) and (9) are

$$\omega^{\pm}(k) = \frac{(\bar{\omega}_1 + \bar{\omega}_2)}{2} \pm \sqrt{\Delta^2 + (g(ka))^2}, \tag{10}$$

$$\chi^{\pm} = (V_0/U_0)^{\pm} = -\frac{\Delta \pm \sqrt{\Delta^2 + (g(ka))^2}}{g(ka)}, \tag{11}$$

where $\Delta = (\bar{\omega}_2 - \bar{\omega}_1)/2$ and $\chi^{\pm}$ are the amplitude ratios corresponding to frequencies $\omega^{\pm}(k)$. Note that $\chi^+\chi^- = -1$, due to the orthogonality of these two eigenmodes at a fixed wavevector k. At a fixed frequency, $\chi^+\chi^-$ is not necessarily equal to -1.

From the electric field distributions of defects in the square and triangular lattices, shown in figure 2, we find that the electric field at the site ($x = 0$, $y = 0$) of the square lattice has the same polarity (sign) as its nearest neighboring site ($x = 0$, $y = 2a$) and the next nearest neighboring site ($x = a$, $y = 2a$). Because $\Delta\varepsilon < 0$ for the air–defect PCWs in both square and triangular lattices, the coupling coefficients α and β are both negative values. Here, we assume $\bar{\omega}_2 > \bar{\omega}_1$ in the following discussion; therefore, we shall call the high frequency PCW2 (low frequency PCW1) waveguide 2 (waveguide 1).

Because $|g(ka)|$ has a maximum value at $k = 0$, one should expect the dispersion curves to have the largest splitting there. As α and β are negative values as discussed before, $g(ka)$ is always a negative value for all k if $|2\beta/\alpha| < 1$, and its value can change from negative to positive as k increases from 0 to π when $|2\beta/\alpha| > 1$. Under this condition, $|2\beta/\alpha| > 1$, the coupler can be decoupled when $g(k_D a) = 0$ at a certain $k = k_D$ and have eigenfrequencies $\omega^+ = \bar{\omega}_2$ and $\omega^- = \bar{\omega}_1$ separately; that is, the field launched in PCW1 will always be confined in PCW1 without being coupled to PCW2, and vice versa. We can simply use the ratio of the maximal field values instead of integrals such as equation (2) to estimate coefficients α, β and $|2\beta/\alpha|$ by assuming the field distribution to be strongly localized near the dielectric rods. Thus, $|2\beta/\alpha| \sim 2E(0, 2a)/E(\pm a, 2a)$ in the square lattice and $\sim 2E(0, \sqrt{3}a)/E(\pm a, \sqrt{3}a)$ in the triangular lattice.

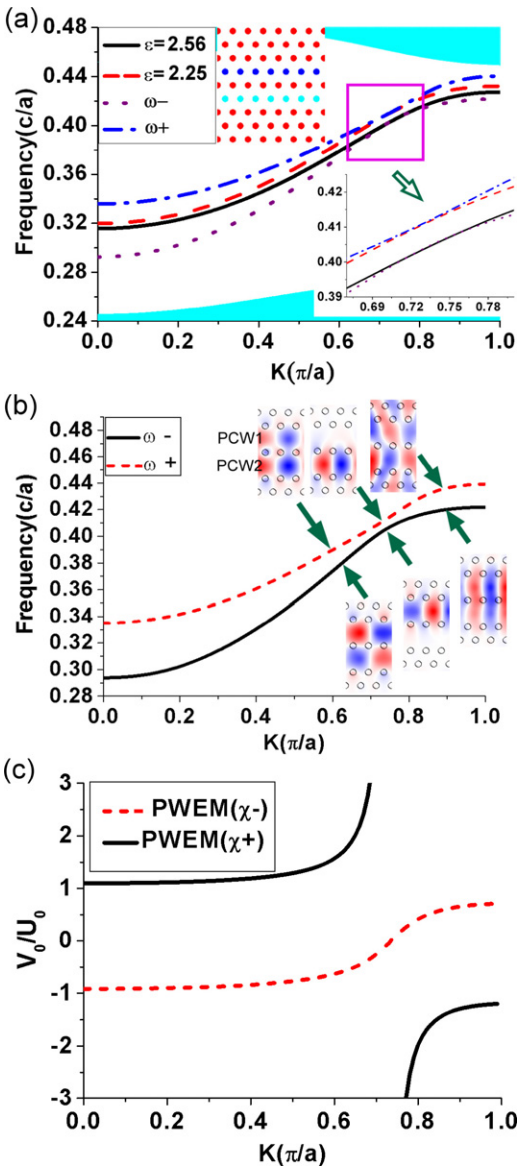

Figure 3. Simulation results from the PWEM. (a) Dispersion relations for two isolated PCWs ($\varepsilon = 2.56$ and $\varepsilon = 2.25$) and the directional coupler in the triangular lattice (shown as the inset). (b) The dispersion curves of the directional coupler and its eigenmode profiles below, above and at the decoupling point. (c) The mode amplitude ratios of the coupler.

Because $g(ka) < 0$ for $0 \leqslant k < k_{\mathrm{D}}$ under the condition $|2\beta/\alpha| > 1$ (or for all k under the condition $|2\beta/\alpha| < 1$), the lower frequency mode (ω^-) has $-1 < \chi^- < 0$; namely, the eigenmode of the coupler displays the PCW1 and PCW2 electric fields not only as out of phase but also concentrated on the low frequency PCW1. This odd-like fundamental (low frequency) mode is called the 'anti-bonding' mode, borrowed from the molecular physics of two atoms. On the other hand, the high frequency and even-like mode called the 'bonding' mode has $\chi^+ > 1$; thus, it is superposed with in-phase electric fields from both PCWs, where the field strength is concentrated on the high frequency PCW2.

However, as $k > k_{\mathrm{D}}$ under the condition $|2\beta/\alpha| > 1$, $g(ka)$ becomes positive and $0 < \chi^- < 1$. The fundamental mode is a bonding mode, which is superposed with the in-phase electric fields from both PCWs, where the field strength is concentrated on the low frequency PCW1. And the high frequency anti-bonding mode with $\chi^+ < -1$ has the field strength concentrated on the high frequency PCW2. We find that the fundamental modes of the asymmetric coupler contain no degenerate state (anti-crossing dispersion relations) and can switch from the anti-bonding to the bonding mode as k varies, crossing the decoupling point k_{D}. As in the previous study on the symmetric coupler [15], we can simply set $\Delta = 0$ to obtain $\chi^{\pm} = \pm 1$ at all k, i.e., the fundamental mode is either odd or even depending upon the sign of $g(ka)$. The dispersion curves of the symmetric coupler can cross at the decoupling point if $|2\beta/\alpha| > 1$. Furthermore, upon increasing the separation of PCWs to two rows apart [22], from equation (2), coupling coefficients α and β become positive values and are smaller than the coupling coefficients of the one-row-separation PCWs. The fundamental mode becomes a bonding mode, and whether or not mode switching will happen is still determined by the criterion $|2\beta/\alpha| > 1$.

In order to prove that the formula derived using TBT can explain phenomena obtained from the PWEM well, we consider as an example a two-dimensional triangular (square) lattice PC made from dielectric rods with dielectric constant $\varepsilon_r = 12$ and radius $= 0.2a$ in the air. Due to the field symmetry, the coupling coefficient ratio β/α is a larger value in the triangular lattice than in the square lattice. It should be easier to reach the criterion $|2\beta/\alpha| \approx 2E(0, 2a)/E(\pm a, 2a) > 1$ for the mode switching behavior in the triangular lattice than in the square lattice, as shown in figure 2(c) [15]. Therefore, we consider a triangular lattice PC, and the line defects forming PCW1 and PCW2 are created by setting the dielectric constants of defect rods at 2.56 and 2.25, respectively. The eigenfrequencies of a point defect with a transverse magnetic field (TM), whose electric field is parallel to the dielectric rods, are $\omega_1 = 0.365\ (2\pi c/a)$ and $\omega_2 = 0.371\ (2\pi c/a)$, respectively, where c is the speed of light in vacuum. The decoupling point is located at $k_{\mathrm{D}} = 0.73\pi/a$ where the eigenfrequencies of the PC couplers decouple in eigenfrequency in single-line-defect PCWs, as shown in figure 3(a). Note that the dispersion curves do not cross in the asymmetric coupler. As shown in figure 3(b), the eigenmode of the high (low) frequency band at wavevector $k < k_{\mathrm{D}}$ is the bonding (anti-bonding) mode, but these modes switch when $k > k_{\mathrm{D}}$; namely, the eigenmode of high (low) frequency band is anti-bonding (bonding). And the electric field is concentrated on PCW2 for the high frequency ($\omega^+(k_{\mathrm{D}})$) mode and on PCW1 for the low frequency ($\omega^-(k_{\mathrm{D}})$) mode at the decoupling point k_{D}. The mode switching phenomenon at k_{D} is shown easily by plotting the ratios of the eigenmodes ($\chi = V_0/U_0$) obtained from the PWEM. We observe that χ changes sign at the decoupling point k_{D} (see figure 3(c)).

3. Electric field distribution and energy transfer

After obtaining the eigenfrequencies (dispersion relations) and eigenvectors (field amplitudes) of the directional coupler, we shall calculate the energy transfer between the coupled PCWs.

If an EM wave with a given frequency propagates in the directional coupler, the wavefunction or field distribution at site n in each of the coupled PCWs can be expressed as the superposition of the eigenmodes of the directional coupler,

$$U_n(na) = A\,\mathrm{e}^{\mathrm{i}k_a na} + B\,\mathrm{e}^{\mathrm{i}k_b na}, \tag{12}$$

$$V_n(na) = A\chi^a\,\mathrm{e}^{\mathrm{i}k_a na} + B\chi^b\,\mathrm{e}^{\mathrm{i}k_b na}, \tag{13}$$

where the propagation constants of the anti-bonding mode k_a and bonding mode k_b and their corresponding amplitude ratios of χ^a and χ^b can be obtained from equations (10) and (11). Note that $\chi^a\chi^b$ is not necessarily equal to -1 for a given frequency because the mode patterns of the directional coupler at a given frequency are not the eigenmodes of the same system. Let $x = na$; one can rewrite equations (12) and (13) as the following continuous equations:

$$U(x) = A\,\mathrm{e}^{\mathrm{i}k_a x} + B\,\mathrm{e}^{\mathrm{i}k_b x}, \tag{14}$$

$$V(x) = A\chi^a\,\mathrm{e}^{\mathrm{i}k_a x} + B\chi^b\,\mathrm{e}^{\mathrm{i}k_b x}. \tag{15}$$

Taking derivatives of $U(x)$ and $V(x)$ with respect to x, we have the coupled PCW equations

$$\frac{\mathrm{d}U(x)}{\mathrm{d}x} = \mathrm{i}M_1U(x) + \mathrm{i}\kappa_{12}V(x), \tag{16}$$

$$\frac{\mathrm{d}V(x)}{\mathrm{d}x} = \mathrm{i}M_2V(x) + \mathrm{i}\kappa_{21}U(x), \tag{17}$$

where $M_1 = (k_a\chi^b - k_b\chi^a)/(\chi^b - \chi^a)$ and $M_2 = (k_a\chi^a - k_b\chi^b)/(\chi^a - \chi^b)$ are the effective propagation constants of PCW1 and PCW2 for the directional coupler, $\kappa_{21} = -\kappa_{12}\chi^b\chi^a$ and $\kappa_{12} = (k_a - k_b)/(\chi^a - \chi^b)$ are the effective coefficients of coupling between PCWs. The solutions of the coupled PCW equations are

$$\begin{bmatrix} U(x) \\ V(x) \end{bmatrix} = \begin{bmatrix} \mathrm{e}^{\mathrm{i}M_1x} & 0 \\ 0 & \mathrm{e}^{\mathrm{i}M_2x} \end{bmatrix} \begin{bmatrix} D_{11}\eta & \mathrm{i}D_{12}\eta \\ \mathrm{i}D_{21}\eta^* & D_{22}\eta^* \end{bmatrix} \begin{bmatrix} U(0) \\ V(0) \end{bmatrix}. \tag{18}$$

Here $U(0)$ and $V(0)$ are the electric field amplitudes at $x = 0$, $D_{12} = (\kappa_{12}\sin(fx))/f$, $D_{21} = (\kappa_{21}\sin(fx))/f$, $D_{11} = D_{22}^* = \cos(fx) - \mathrm{i}\delta\sin(fx)/f$, and $\eta = \exp(\mathrm{i}\delta x)$, with $f = (k_a - k_b)/2$ and $\delta = f(\chi^a + \chi^b)/(\chi^a - \chi^b)$. The maximum energy transferred from PCW1 to PCW2 is proportional to $|\kappa_{21}/f|^2 = 4(\chi^b\chi^a)^2/(\chi^b - \chi^a)^2$ and that transferred from PCW2 to PCW1 is proportional to $|\kappa_{12}/f|^2 = 4/(\chi^b - \chi^a)^2$. There are maximum energy transfers into the other waveguides at $fx = \pi/2$, so the coupling length is defined as $\pi/|k_a - k_b|$. There are no crossing points in asymmetric PCWs, as the coupling length would not be infinite by TBT, as shown in figure 4(a), but the lower energy transfer is still around the decoupling points. The energy will transfer completely into the other waveguide only in symmetric ones because this happens only at $\delta = 0$.

For an incident wave frequency ω, the wavevector k_a for the anti-bonding mode should be larger than k_b for the bonding mode for $k < k_D$. Since $|\chi^a|$ is smaller for large wavevectors, if we denote the mode ratio of the lower frequency band at k_b as $\chi^a(k_b)$, we have $|\chi^b\chi^a| \leqslant |\chi^b\chi^a(k_b)| = 1$ and $4(\chi^b\chi^a)^2/(\chi^b - \chi^a)^2 \leqslant 4/(\chi^b - \chi^a)^2$ and $\leqslant 1$, as shown in figures 4(b) and (c), which is obtained from the PWEM. Therefore, the maximum energy transferred from PCW1 to PCW2 should be smaller than that transferred from PCW2 to PCW1. However $|\kappa_{12}/f|^2$ can be larger than 1, meaning that the output peak energy can be larger than the input peak energy. This comes from the different field localizations of the eigenmodes.

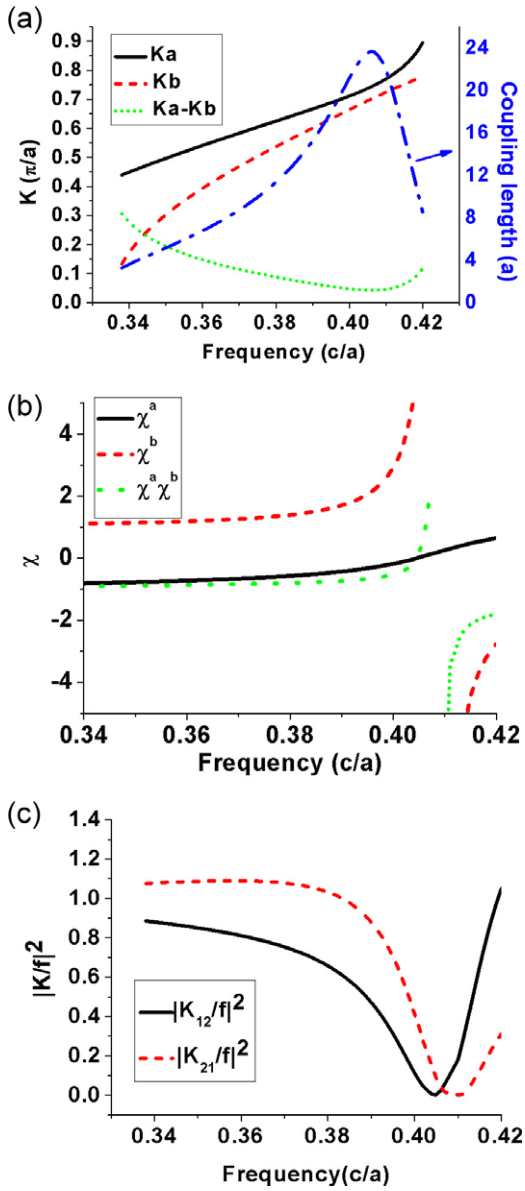

Figure 4. (a) The wavevectors of the bonding and anti-bonding modes and the coupling length of the PC couplers for different frequencies. (b) The mode amplitude ratio ($\chi = V_0/U_0$) of the bonding and anti-bonding modes. (c) The ratios of the maximum energy transferred from PCW2 to PCW1 ($|k_{12}/f|^2$) and from PCW1 to PCW2 ($|k_{21}/f|^2$).

4. Conclusion

We have extended the TBT to study asymmetric couplings between two non-identical line defect photonic waveguides. By considering the coupling between two waveguides beyond

the nearest neighboring approximation, analytic expressions for the dispersion relations and eigenmode ratios of an asymmetric photonic crystal coupler agree well with the phenomena calculated using PWEM results. Due to the symmetry breaking, these two dispersion curves will never cross, even with the criterion $|2\beta| > |\alpha|$ obeyed. Nevertheless, as the symmetric coupler shows, the eigenmode patterns, which are the bonding and anti-bonding modes, do switch on the same dispersion curves when wavevector k varies across the decoupling point. At the higher (lower) frequency of the dispersion relation curve, the electric field distribution of the eigenmodes would localize mainly at the PC waveguide with a higher (lower) eigenfrequency, which corresponds to an incomplete EM field transformation between two waveguides. For a given incident frequency, the electric field distributions and energy transfer of the coupler can be expressed analytically by using the wavevector and derived amplitude ratios of the bonding and anti-bonding modes. The coupling length at the decoupling point is no longer infinite, but low energy transfer occurs around there. Although complete energy transfer into the other waveguides is impossible in asymmetric waveguides, the peak power in the output dielectric rods can be larger than that in the input ones due to the electric fields having different strengths of electric field localization in each of the waveguides.

Acknowledgments

We acknowledge partial financial support from the National Science Council (NSC) of the Republic of China under Contract Nos NSC96-2628-M-009-001-MY3, NSC96-2112-M-034-002-MY3, and NSC96-2628-E-009-018-MY3. Mr Chih-Hsien Huang would like to thank the NSC for providing a fellowship.

References

[1] Meade R D, Devenyi A, Joannopoulos J D, Alerhand O L, Smith D A and Kash K 1994 *J. Appl. Phys.* **75** 4753
[2] Mekis A, Chen J C, Kurland I, Fan S, Villeneuve P R and Joannopoulos J D 1996 *Phys. Rev. Lett.* **77** 3787
[3] Qiu M, Mulot M, Swillo M, Anand S, Jaskorzynska B, Karlsson A, Kamp M and Frochel A 2003 *Appl. Phys. Lett.* **83** 5121
[4] Sharkawy A, Shouyuan S, Prather D W and Soref R A 2002 *Opt. Express* **10** 1048
[5] Nagpal Y and Sinha R 2004 *Microw. Opt. Technol. Lett.* **43** 47
[6] Leung K M and Liu Y F 1990 *Phys. Rev. Lett.* **65** 2646
[7] Johnson S G and Joannopoulos J D 2001 *Opt. Express* **8** 173
[8] Johnson S G, Mekis A, Fan J and Joannopoulos J D 2001 *Comput. Sci. Eng.* **3** 38
[9] Taflove A 1995 *Computational Electrodynamics: The Finite-Difference Time-Domain Method* (Boston: Artech House)
[10] Benisty H 1996 *J. Appl. Phys.* **79** 7483
[11] Qiu M 2001 *Microw. Opt. Technol. Lett.* **30** 327
[12] Guven K and Ozbay E 2005 *Phys. Rev.* B **71** 085108
[13] Mingaleev S F and Kivshar Y S 2002 *J. Opt. Soc. Am.* B **19** 2241
[14] Vicencio R A and Johansson M 2006 *Phys. Rev.* E **73** 046602
[15] Chien F S S, Tu J B, Hsieh W F and Cheng S C 2007 *Phys. Rev.* B **75** 125113
[16] Chien F S S, Hsu Y J, Hsieh W F and Cheng S C 2004 *Opt. Express* **12** 1119
[17] Chien F S S, Cheng S C, Hsu Y J and Hsieh W F 2006 *Opt. Commun.* **266** 592
[18] Bayindir M, Temelkuran B and Ozbay E 2000 *Phys. Rev. Lett.* **84** 2140
[19] Yariv A, Xu Y, Lee R K and Scherer A 1999 *Opt. Lett.* **24** 711
[20] Joannopoulos J D, Johnson S G, Winn J N and Meade R D 2008 *Photonic Crystal: Molding the Flow of Light* 2 edn (New Jersey: Princeton University Press)
[21] Christodoulides D N and Efremidis N K 2002 *Opt. Lett.* **27** 568
[22] Koponen T, Huttunen A and Törmä P 2004 *J. Appl. Phys.* **96** 4039